PCCP

Accepted Manuscript




ROYAL SOCIETY OF CHEMISTRY

www.rsc.org/pccp

Cite this: DOI: 10.1039/c0xx00000x

www.rsc.org/xxxxxx

**Paper**

# Modulation of ultrafast photoinduced electron transfer in H-bonding environment: PET from aniline to coumarin 153 in the presence of an inert co-solvent cyclohexane

**Nabajeet Barman, Tousif Hossen, Koushik Mondal and Kalyanasis Sahu***

***Received (in XXX, XXX) Xth XXXXXXXXX 20XX, Accepted Xth XXXXXXXXX 20XX***
**DOI: 10.1039/b000000x**

Despite of intensive research, the role of H-bonding environment on ultrafast PET remains illusive. For example, Coumarin 153 (C153) undergoes ultrafast photoinduced electron transfer (PET) in electron-donating solvents, in both aniline (AN) and *N,N*-dimethylaniline (DMA), despite of their very different H-bonding abilities. Thus, donor-acceptor (AN-C153) H-bonding may have only a minor role on PET (Yoshihara and co-workers, *J. Phys. Chem. A*, 1998, **102,** 3089). However, donor-acceptor H-bonding may be somehow less effective in the neat H-bonding environment but could become dominant in the presence of an inert solvent (*Phys. Chem. Chem. Phys.*, 2014, **16,** 6159). We successfully applied and tested the proposal here. The nature of PET modulation of C153 in the presence of a passive component cyclohexane is found to be very different for aniline and DMA. On the addition of cyclohexane to DMA, the PET process gradually becomes retarded but in the case of AN, PET rate was indeed found to be accelerated at some intermediate composition (mole fraction of aniline, $X_{AN}$ ~0.74) compared to that of neat aniline. It is intuitive that cyclohexane may replace some of the donors (AN or DMA) from the vicinity of the acceptor and thus, should disfavour PET. However, in the hydrogen bonding environment using molecular dynamics simulation, for the first time, we show that the average number of aniline molecules orienting its N–H group in the proximity of the C=O group of C153 is actually higher at the intermediate mole fraction (0.74) of aniline in the mixture rather than in neat aniline. This small but finite excess of C153-AN H-bonding already present in the ground state may possibly account for the anomalous effect. The TD-DFT calculations presented here showed that the intermolecular H-bonding between C153 and AN strengthens from 21.1 kJ $mole^{-1}$ in the ground state to 33.0 kJ $mole^{-1}$ in the excited state and consequently, H-bonding may assist PET according to the Zhao and Han model. Thus, we not only justify both the theoretical prediction (efficient H-bond assisted PET within C153-AN pair) and experimental observation (minor H-bond assisted PET in neat solvent) but also established our previous hypothesis that an inert co-solvent can enhance the effect of H-bonding from molecular insights.

## 1 Introduction

Does H-bonding play a key role in guiding ultrafast electron transfer (ET) other than just maintaining the donor-acceptor (D-A) proximity? The question is of outmost importance for comprehensive understanding of electron transfer within H-bonded scaffold prevalent in various chemical and biological systems.[1-4] Usually, insight on H-bonding influence is seek from comparing photoinduced electron transfer (PET) dynamics of dissolved acceptors (e.g. coumarin fluorophores) in the neat electron donating solvents with differing H-bonding ability (e.g. aniline (AN) vs. *N,N*-dimethylaniline (DMA)). An acceptor dissolved in neat electron-donating solvent is expected to be surrounded by several donors and hence, the proximity of D-A is guaranteed regardless of any specific donor-acceptor interaction e.g. H-bonding. Thus, donor-acceptor closest approach may be similar in both cases (AN and DMA) and hence, PET rate variation in the two systems may possibly hint at any other effect of H-bonding on PET rather than just controlling the donor-acceptor proximity.[5-6] Yoshihara and co-workers studied PET of a series of coumarin fluorophores in neat AN and DMA solvents.[7] They found faster PET in DMA than in AN for all coumarins, which they attributed to the better electron donating ability of DMA compared to AN (oxidation potentials of AN and DMA in acetonitrile are 0.93 and 0.76V vs. SCE, respectively[7]). H/D kinetic isotope effect is another indication of H-bonding involvement on PET. The H/D kinetic isotope effect was significant for slower PET but only a minor effect was observed for faster PET dynamics. Most recently, Nibbering and coworkers found that PET dynamics of coumarin 337 (C337) dissolved in several aromatic amines (AN, mono and dimethyl-aniline) remained unchanged irrespective of the H-bonding ability of the amine solvents and have not observed any isotope effect.[8] They concluded that H-bonding has insignificant influence on PET.

However, recent time-dependent density functional theory (TD-DFT) calculations by Zhao and Han claimed that the

intermolecular H-bonding between coumarin 102 (C102) and H-bonding donors (e.g. phenol) becomes stronger in the excited state and predicted that such strengthening could be significant on inducing PET within H-bonded donor-acceptor pairs.[9-11] Following them, Liu and coworkers reported that the excited-state H-bond strengthening formalism may be applied to PET between coumarin dyes (C102 and C337) and H-bonded AN donors.[12-14] They proposed a H-bonding assisted PET mechanism via internal conversion from a locally excited (LE) state to a charge transfer (CT) state consistent with the original proposal of Zhao and Han as a consequence of strengthening of intermolecular H-bond in the electronically excited state.[9, 11, 15-16]

Thus, a minor to moderate H-bonding effect on PET has been observed in previous experiments, while a strong effect of H-bonding was increasingly demanded from theoretical calculations. To resolve this inconsistency, we recently conjectured that the effect of H-bonding required to enhance PET may be suppressed in neat AN possibly because of competitive nature of the donor-acceptor (D-A) and donor-donor (D-D) H-bonding (Scheme 1).[17-18] Note that the intermolecular H-bonding of the type N-H···N has been reported for aniline solutions[19] and aniline clusters.[20] However, the competitive H-bonding situation may break down drastically in the presence of an inert component. Apparently, a third component that cannot participate either in H-bonding or in electron transfer should merely replace some of the donor molecules from the vicinity of the acceptor (scheme 1) and thus may retard the PET event.[17-18] It was reported by Castner et al. that chlorobenzene (a non-interacting component) retards PET of coumarin acceptors (C151 or C152) dissolved in neat DMA.[21] Very recently, Letrun et al. reported that the number of DMA around coumarin varies in mixed solvent.[22] However, we observed that in the presence of a non-interacting component (cyclohexane or toluene) the PET of C102 dissolved in AN gets accelerated at an intermediate mole fraction in the mixture compared to neat aniline.[17-18] The D-D H-bonding which may possibly resist the D-A (AN-C102) H-bonding to attain optimum conformation for PET in neat H-bonding solvent, could be disrupted by the inert component. The breakdown of D-D hydrogen bonding network may assist the key D-A H-bond to exert its favorable influence on PET.[18] Similar observation was also noted for a C102-phenol system.[5] However, it was just a speculation to rationalize the experimental observations. It lacks actual molecular insights about the arrangement of donors around the acceptor at different composition and thus information on the donor-acceptor H-bonding. Moreover, the acceptor C102 is not a good candidate for ultrafast PET. It is usually reluctant to undergo PET in the absence of H-bonding. This is evident from the fact that no PET occurs for C102 dissolved in neat DMA.[23] A more demanding system is one where there is possibility of H-bond mediated PET operating along with non-H-bonded PET. In that case, competition between H-bonded vs. non-H-bonded PET channels may be interesting.

In this work, we have selected coumarin 153 (C153) as an acceptor which is well known to undergo ultrafast PET in both neat AN and DMA.[7, 24-25] Structurally, C153 is analogous to C102; only the methyl group is substituted by trifluoromethyl group.[26] The $-CF_3$ substitution has a profound effect on the reduction potential and hence, the free energy of electron transfer becomes much more favorable in the case of C153 compared to C102.[7] Thus, normal (non-H-bonded) PET which is not allowed for C102 is highly favorable for C153 as evident from ultrafast PET dynamics in DMA.[7] Here, we have studied PET of excited C153 in the DMA/cyclohexane and AN/cyclohexane mixtures. Similar to C102, the >C=O group of C153 is expected to form H-bonding with the amine hydrogen of AN.

In this article, we have shown the followings. First, we applied steady-state and time-resolved fluorescence to show that the incorporation of inert component (cyclohexane) can modulate PET differentially for AN and DMA. Then, using combination of Fourier transformed infrared (FT-IR) spectroscopy and density functional theory (DFT) calculation, ground-state intermolecular H-bonding between C153 and AN is investigated. Then, we present results from time dependent DFT (TDDFT) calculation to determine the intermolecular H-bonding properties in the excited state and discuss the applicability of the Zhao and Han model in assisting PET. Finally, we will support our hypothesis that inert component may enhance the donor-acceptor H-bonding through a MD simulation mimicking the experimental systems. Until now, we have applied the strategy of passive solvent addition to enhance the effect of H-bonding to initiate PET for the C102 systems only. This is the first study which will show that such concepts may be applied for the systems where PET is already ultrafast.

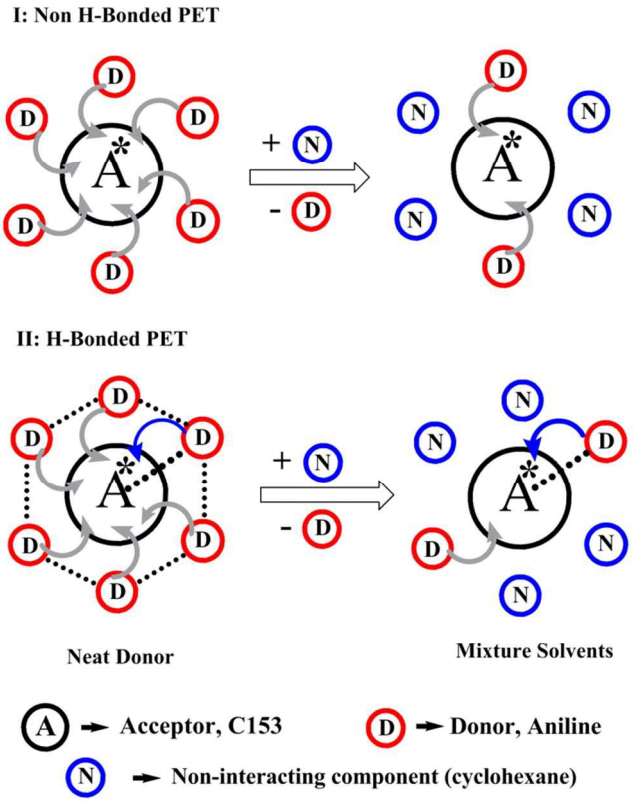


**Scheme 1** Addition of inert co-solvent leads to different modulation of PET depending on the H-bonding ability of the donor. Gray and blue arrows indicate non-H-bonded and H-bonded PET, respectively. In the mixture, H-bonded PET dominates while non-H-bonded PET diminishes.

## 2 Experimental and theoretical methods

**Chemicals.** Coumarin 153 (C153), aniline (AN) and *N*,*N*-dimethylaniline (DMA) were purchased from Sigma-Aldrich. Cyclohexane (HPLC grade) was obtained from Rankem, India.

**Instruments used.** Absorption and emission spectra were recorded on a Perkin-Elmer Lamda-750 spectrophotometer and Jobin-Yvon FluoroMax4 spectrofluorometer, respectively. Fluorescence measurements of C153 in aniline-cyclohexane and DMA-cyclohexane mixtures were performed at an excitation

wavelength of 405 nm. The fluorescence up-conversion experiments were performed on a FOG 100, (CDP) at the laboratory of Prof. Kankan Bhattacharya at Indian Association for the Cultivation of Science, Kolkata, India and details of the set up was already mentioned elsewhere.[27-28] The samples were excited at 405 nm, and emission was monitored at respective emission maxima. FT-IR spectra of C153 were recorded in a Perkin-Elmer Spectrum Two FTIR spectrophotometer.

**DFT and TD-DFT calculations.** The ground state structures of C153, aniline and 1:1 C153-aniline complexes were optimized by DFT method using B3LYP functional and 6-311+G(d,p) basis set in gas phase. The optimizations were further confirmed by the absence of imaginary frequency in subsequent frequency calculations. The excited state optimizations were performed by TD-DFT calculations employing the same hybrid functional and basis set. All the calculations were done using Gaussian 09 package.[29]

**MD simulations.** To perform the MD simulation, the ground-state structures of C153, aniline and cyclohexane were optimized using B3LYP/6-31G* level of theory in Gaussian 03W.[29] To obtain the partial charges, we use population analysis of Merz-Singh-Kollman using HF/6-31G* level followed by RESP charge fitting.[30] The initial structures were packed in a cubic box of dimension 42Å ×42Å×42Å by placing a single coumarin (C153) unit at the center while placing the solvent entities randomly using packmol[31] package so that minimum tolerance between two units is 2Å. The compositions of different mixtures used for simulation are given in supporting information (Table S1). The simulation was performed in AMBER12[32] program suit using generalized amber force field (GAFF) parameters.[33] GAFF force field has been proven to be satisfactory to reproduce properties of small organic molecules including aniline and cyclohexane.[34] To avoid bad van der Waals contacts on the initial structures, energy minimization for 500 steps with first 200 steps in steepest descent method followed by 300 steps in conjugate gradient method were performed. Subsequently, each system was heated slowly 300K in 20 ps in canonical (NVT) ensemble maintaining weak restraints (force constant = 1.0 kcal $mol^{-1}$ $Å^{-2}$) over all atoms. For temperature regulation, we use the Langevin thermostat with a collision frequency of 2 $ps^{-1}$. Then, the systems were equilibrated in isothermal−isobaric (NPT) ensemble without any restraint for 400 ps at atmospheric pressure. Finally, a 20 ns production run was carried out in NPT ensemble at 1 atm pressure. To maintain the pressure, Berendsen barostat was used with a pressure relaxation time of 2 ps. A cutoff distance of 10 Å was applied for all non-bonding interactions and the long-range electrostatic interactions were treated using the particle mesh Ewald (PME) method. The bonds involving hydrogen atoms were constrained by using SHAKE algorithm[35] and periodic boundary condition was used. Snapshots were saved after every 1 ps. The post-analysis of the simulation trajectories was done either in the ptraj/cpptraj module of AMBER12 or in VMD package.[36] The energy and density of the system remain consistent over the entire production run ensuring stability of the system. The average density of the system containing neat aniline and neat cyclohexane were 0.760 and 1.022 g/cc, respectively close to their reported densities of 0.779 and 1.067 g/cc (see ESI, Fig. S1).

## 3 Results

***3.1. Steady State Measurements.*** Fig. 1 shows the absorption spectra of C153 in the AN-cyclohexane mixtures at different mole fractions of AN. Absorption spectrum of C153 in the mixture exhibits gradual red-shift with increase of the mole fraction of AN. This significant red-shift in the absorption maximum may be due to C153-AN H-bond formation and increase in the average polarity of the medium. The extent of red-shift is comparatively less in DMA-cyclohexane mixtures possibly because of the absence of H-bonding between C153 and DMA (see ESI, Fig. S2).

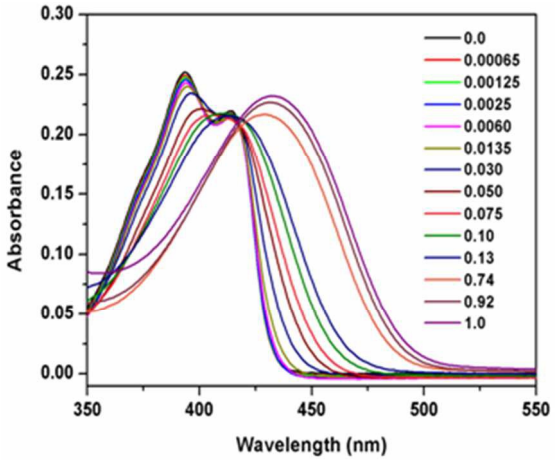


**Fig. 1** Absorption spectra of C153 in cyclohexane-AN mixtures at different mole fractions of the electron donor (AN). Absorption spectra exhibit red-shift with increase of the mole fraction of donor.

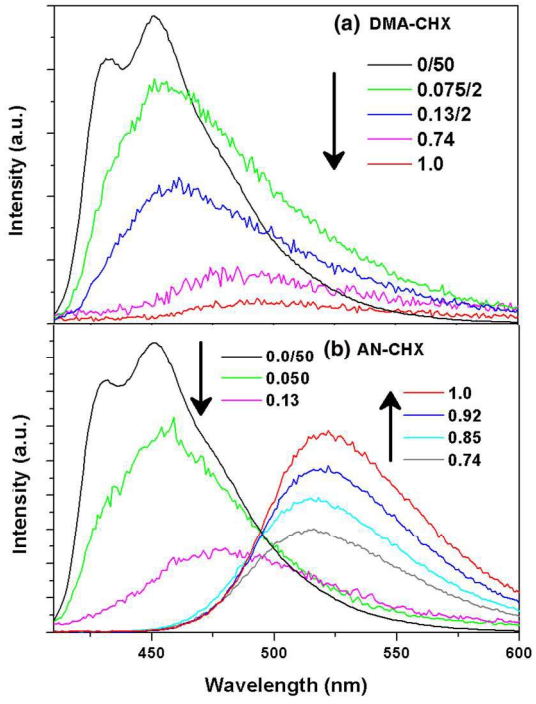


**Fig. 2** Steady-state emission spectra of C153 in (a) cyclohexane-DMA and (b) cyclohexane-AN mixtures at different mole fractions of the electron donor (DMA or AN). Emission intensity of C153 gradually diminishes on the addition of DMA solvent but shows an anomalous trend in the case of aniline. The emission spectrum of C153 in neat cyclohexane is divided by 50 and in DMA-cyclohexane mixtures at 0.075 and 0.13 mole fractions are divided by 2 to scale it down for comparison.

C153 shows very strong emission in cyclohexane (quantum yield (QY) close to unity)[37] but the fluorescence becomes strongly quenched in neat AN or DMA. The extent of reduction of fluorescence intensity is more severe in DMA than in AN. This is in accordance with the better electron donating ability of DMA compared to AN (oxidation potentials of AN and DMA in acetonitrile are 0.93 V and 0.76 V vs. SCE, respectively[7]). Gradual addition of DMA to C153 dissolved in cyclohexane results in a continuous decrease of the emission intensity and a regular red-shifting of the emission maxima (Fig. 2a). The shift in the emission maximum of C153 is indicative of the polarity variation in the mixture while the quenching of the fluorescence is due to PET from the donor solvent (DMA) to the excited C153. However, in the cyclohexane-AN mixtures, the variation of quantum yield does not show a monotonous trend (Fig. 2b). The QY first reduces with increase of the mole fraction of AN ($X_{AN}$) in the low concentration regime ($X_{AN} < 0.13$) but the trend reversed at higher mole fraction region ($X_{AN} > 0.74$); the QY increases with addition of more AN. Note that QY was similar at $X_{AN} = 0.13$ and 0.74. Note that we could not perform experiment in between this range due to mutual insolubility of the components at room temperature (298 K). The QY at $X_{AN} = 0.13$ is found to be ~120 times lower than that in neat cyclohexane and nearly two times less compared to neat AN. Thus, the variation of quantum yield was anomalous i.e. more efficient quenching was observed at some intermediate mole fraction rather than in neat aniline. However, due to immiscibility, the accurate determination of the maximum quenching point was not possible. Note that for C102, we observed similar anomalous quenching in AN-cyclohexane mixture with maximum quenching at $X_{AN} = 0.075$.[17]

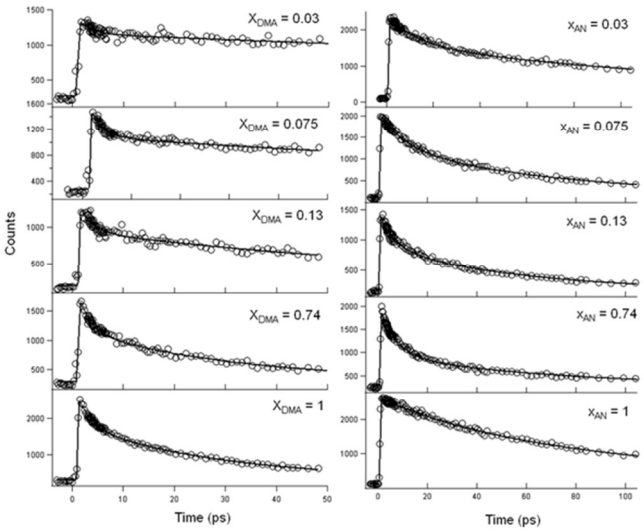


**Fig. 3** The fluorescence decays of C153 in (a) cyclohexane-DMA (left panel) and (b) cyclohexane-AN (right panel) mixtures at different mole fractions of the electron donor (DMA/AN). Clearly as the amount of DMA increases, PET becomes faster and reaches the optimum value in neat DMA. Interestingly, for cyclohexane-AN mixture, PET becomes faster at intermediate $X_{AN}$ compared to neat AN

***3.2. Time Resolved Measurements.*** The fluorescence up-conversion measurements were carried out to probe the ultrafast decays of the fluorescent acceptor in the donor-inert solvent mixtures at some specific mole fractions (Fig. 3). All the decay components were found to be bi-exponential (Table 1). In the cyclohexane-DMA mixtures, magnitude of the fast (2.4 - 2.8 ps) component remains almost invariant to the amount of donor while its contribution increases at higher mole fractions. The other decay component gradually decreases (from 285 ps at $X_{DMA} = 0.03$ to 28 ps in neat DMA) with increase in the mole fraction of the donor (DMA) in the mixture. The origin of the two components is not clearly understood. One possibility may be that many different solvent arrangements around the acceptor may be possible with varying number and orientation of the donors. The faster component may be assigned to the PET from an arrangement where several donors are already pre-organized in the vicinity of the excited acceptor, while the slower component may arise from a case where less numbers of donor molecules or less organized donors are present around the acceptor. In the first case, electronic coupling may be stronger than in the second case. The relative probability of the two arrangements may vary with the composition of the mixture. Vauthey and co-workers reported excitation wavelength dependent PET dynamics of coumarins due to heterogeneous distribution of donor molecules around the acceptor.[22] In cyclohexane-DMA mixture, the average fluorescence lifetime of C153 decreases with increase in the mole fraction of DMA. This was in agreement with the observation of regular reduction of emission quenching with mole fraction. The most interesting observation is that in cyclohexane-AN mixture, the average fluorescence lifetime initially decreases with increase in $X_{AN}$ (very short average lifetime at $X_{AN} = 0.74$) and thereafter, increases with further increase in $X_{AN}$. The fast component (6-35 ps) may be assigned to PET within the C153-AN H-bonded complex and its contribution is found to be maximum at $X_{AN} = 0.74$ (Table 1). Thus, both steady-state and time-resolved fluorescence results collectively indicate more facile H-bonded PET at an intermediate mole fraction ($X_{AN} = 0.74$) rather than in neat AN.

**Table 1** Fluorescence decay components of coumarin 153 (C153) in the cyclohexane-AN and cyclohexane-DMA mixtures at different mole fractions of the donors (DMA or AN). Excitation wavelength was at 405 nm and emission was measured at respective emission maxima.

| Donor | $X_{Donor}$ | QY | Lifetimes (τ/ps) | | |
|---|---|---|---|---|---|
| | | (φ) | $\tau_1$ ($a_1$) | $\tau_2$ ($a_2$) | ⟨τ⟩ |
| DMA | 0.03 | 0.055 | 2.6 (0.19) | 285 (0.81) | 232 |
| | 0.075 | 0.040 | 2.5 (0.36) | 147 (0.64) | 95 |
| | 0.13 | 0.027 | 2.7 (0.34) | 90 (0.66) | 60 |
| | 0.74 | 0.006 | 2.4 (0.40) | 31 (0.60) | 20 |
| | 1.00 | 0.003 | 2.8 (0.36) | 28 (0.64) | 19 |
| AN | 0.03 | 0.040 | 13 (0.33) | 165 (0.67) | 115 |
| | 0.075 | 0.023 | 10 (0.40) | 75 (0.60) | 49 |
| | 0.13 | 0.007 | 6 (0.40) | 53 (0.60) | 34 |
| | 0.74 | 0.008 | 7 (0.58) | 67 (0.42) | 32 |
| | 1.00 | 0.015 | 35 (0.26) | 120 (0.74) | 96 |

***3.4. Fourier transformed infrared (FTIR) spectroscopy.***

To get an idea of the H-bonding nature of C153 in aniline-cyclohexane mixtures, FT-IR spectra were recorded for the C=O stretching region of C153 (see ESI, Fig. S3). In neat cyclohexane, the C=O stretch of C153 was found to be at 1748 $cm^{-1}$, which is characteristics of the stretching frequency of an unbound C=O group. In the cyclohexane-aniline mixture, the strength of the absorption band at 1748 $cm^{-1}$ decreases with increase in $X_{AN}$ and an additional band develops at 1736 $cm^{-1}$. This new band may be due to lowering of the stretching frequency of the carbonyl group of C153 in the H-bonded complex. The intensity of the band at 1736 $cm^{-1}$ gradually increases with increase of the mole fraction of aniline. However, the C=O stretching vibration (mainly at $X_{AN} = 0.74$ and in neat AN) is overlapped with some other vibration mode of aniline (possibly arising due to aniline-aniline association[23]). Hence, a very conclusive remark about the H-

bonding condition at higher mole fractions can not be inferred from the FTIR measurement.

### *3.4. DFT and TD-DFT calculations.*

The ground state optimized structure of the C153-AN complex showed that the carbonyl group of C153 is hydrogen bonded with the N-H group of aniline (see ESI, Fig. S4). The H-bond distance was found to be 2.098 Å and the H-bond energy was calculated to be 21.14 kJ $mol^{-1}$. To get an idea about the nature of the electronic transitions involved in the free C153 and C153-AN complexes single point or Frank-Condon (FC) TDDFT calculations were performed. It was found that the $S_2$ state has the highest oscillator strength for the H-bonded complex comparable to the $S_1$ state of free C153 (see ESI, Table S2). Thus, it may be assumed that electronic excitation promotes the complex into the $S_2$ state. The molecular orbital indicates that this transition is locally excited (LE) type with the electron density predominantly localized on coumarin unit (see ESI, Fig. S5). The lowest lying excited state ($S_1$) is of charge transfer (CT) character. These findings are in agreement to the case of C102-AN complex reported previously.[12] To understate the properties of H-bonding in the excited state of the complex, we further optimized the $S_2$ excited state by TDDFT method. The results revealed that the H-bonding becomes stronger in the excited state. The H-bond energy increases to 33.0 kJ $mol^{-1}$ in the excited state, while the H-bonding length is also shorted to 2.006 Å. Thus, we observed excited state H-bond strengthening of the intermolecular H-bond between C153 and AN. As of the C102-AN system,[12] the LE to CT transitions may be possible within the excited H-bonded complex assisting PET.

***3.5. Molecular dynamics (MD) simulations.*** To get a microscopic view of the actual arrangement of donor and the co-solvent molecules around the acceptor, we performed molecular dynamics (MD) simulation. We took a single acceptor in a cubic box containing different numbers of aniline and cyclohexane molecules consistent with the composition of the systems for which fluorescence transients were recorded (see supporting information, Table S2). Several important findings were obtained from the simulation results. From the visual inspection of the MD snapshots (Fig. 4), it is clear that solvent arrangement around C153 is highly anisotropic in nature. The AN molecules are mostly populated around the C=O site of C153 and depleted from other parts of the acceptor.

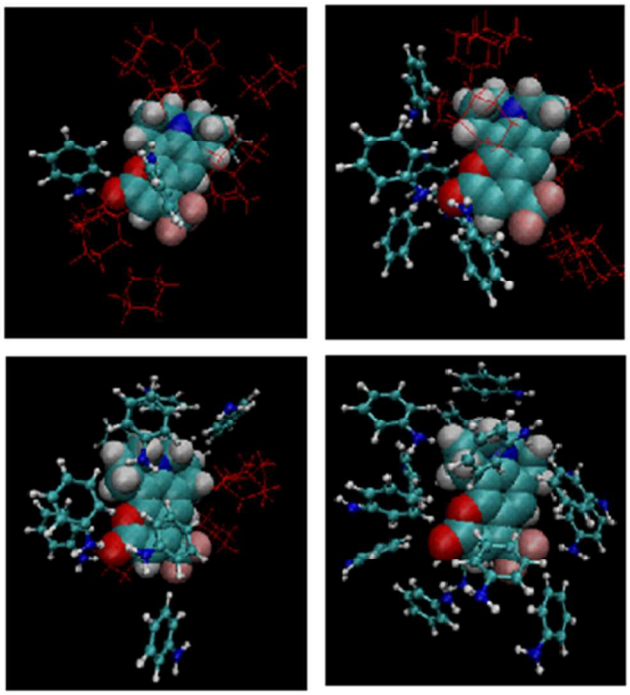

**Fig. 4** Representative MD snapshots showing arrangement of solvents within 3.5 Å of the acceptor C153 at mole fractions- 0.05 (top, left), 0.13 (top, right), 0.74 (bottom, left) and 1.0 (bottom, right). It is clear that aniline (CPK representation) molecules mostly situated near the carbonyl group of C153, while cyclohexane (red) molecules prefer other hydrophobic sites.

The radial distribution function (rdf, g(r)) of the distance between a particular site of the acceptor C153 and a specific atom of the solvent may conveniently represent the arrangement of the solvents (donor or non-interacting co-solvent) around the acceptor. For, this purpose, we chose all possible H-bond accepting sites of C153 - the carbonyl oxygen (O2), the ring oxygen (O1), tertiary nitrogen (N1) and the fluorine (F1-3) atoms. For aniline, we selected either the nitrogen (N1) atom or the two hydrogen (H6 or H7) atoms of the amine group while any one pair of the 12 H atoms were chosen for cyclohexane (molecular structures with atom assignments are supplied in the ESI, Fig. S6. The rdf between O2 of C153 and N1 of AN, g(rO2..N1) displays a very strong peak at 3 Å at all mole fractions (Fig. 5). However the peak strength depends strongly on $X_{AN}$. A very strong peak at $X_{AN}$ = 0.05 indicates much higher probability of finding an AN molecule (facing its N atom towards C=O group) close to C153 than expected from average number density at this mole fraction. The difference of the local density from average density reduces with increase in $X_{AN}$. The enrichment of the polar component in the neighbourhood of the carbonyl site may be due to the dipole-dipole or H-bonding interaction. The rdf between the O2 of C153 and the polar Hs of aniline shows a strong peak at ~2 Å which further emphasizes the possibility of H-bonding formation (Fig. 5). Rdf for other H-bonding sites (O1, N1, F1) of C153 do not show such strong peaks at short distances confirming that the carbonyl oxygen (O2) is the main H-bond accepting site in C153 (see ESI, Fig. S7). The rdf between the O2 of C153 and H atom of cyclohexane shows a depletion near the carbonyl group (see ESI, Fig. S8). This reduction of local density of cyclohexane complements

enrichment of aniline in the carbonyl region of C153.

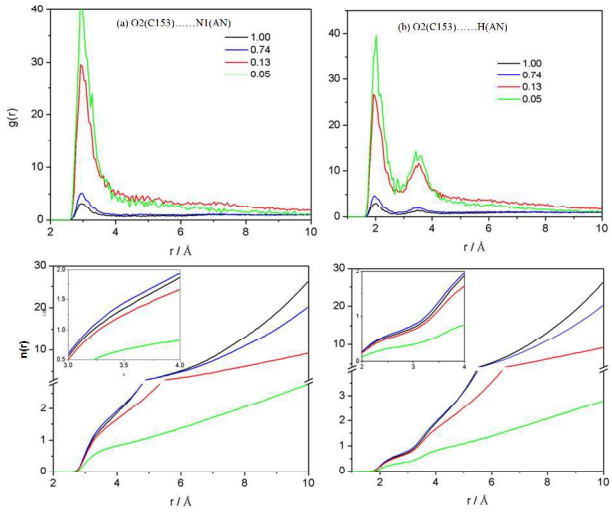


**Fig. 5** The radial distribution function, g(r) of the distance between the carbonyl oxygen (O2) of C153 and (a) the nitrogen atom (N1) of aniline; (b) g(r) between the O2 of C153 and the H (average of H6 and H7) atoms of aniline. The corresponding integrated number n(r) are shown for the two cases in the bottom panels, respectively. The inset shows that the number of aniline molecules in the close proximity of C=O group of C153 is higher at $X_{AN}$ = 0.74 compared to neat aniline.

Note that a change in mole fraction of aniline (or cyclohexane) simultaneously alters the local density of species around the acceptor and also its average number density. A better estimate that can give the number, $n_i(r')$, of a particular solvent (*i*) present within a specified distance r′ from a defined site (α) of the acceptor may be defined as

$$n_i(r')=4\pi\rho_i \int_0^{r'} g_{\alpha i}(r)r^2dr \qquad (1)$$

where $\rho_i$ is the average number density of the solvent *i* in the system. The average number of aniline with its N atom present close (say within 4 Å) to the carbonyl site of C153 varies anomalously with $X_{AN}$ (Fig. 5). The number of aniline molecules in the vicinity of the carbonyl site of C153 is actually higher at $X_{AN}$ = 0.74 than in neat aniline. These aniline molecules, due to its proximity may be important for H-bonding and PET events. Hence, the observed enhancement of PET at 0.74 mole fraction is possibly due to the greater H-bonding in the mixture at intermediate mole fraction than in the neat aniline.

We further calculated the probability (percentage of occupancy) of hydrogen bond formation between the carbonyl oxygen of C153 with amine group of AN at different compositions of the mixtures (Table 2). For this, we use a distance cut off of 3.0 Å and angle cut off of 135°. The most important result is that the H-bonding at $X_{AN}$ = 0.74 is more favourable compared to neat aniline; the occupancy (i.e. percentage of frames that involves D-A H-bonding) was calculated to be 47.1% and 44.5% at 0.74 mole fraction and in neat aniline, respectively. Thus, the result indicates that in the presence of the co-solvent, D-A H-bonding actually favoured and the finite excess of H-bonding found at 0.74 mole fraction may be responsible for the PET acceleration.

We also investigate the effect of the co-solvent on AN-AN H-bonding. It is found that the average number of D-D H-bonding decreases rapidly in the presence of higher amount of cyclohexane (Fig. 6 and Table 2).

**Table 2** The H-bonding parameters obtained from MD simulations at different mole fractions of aniline in the aniline-cyclohexane mixtures using 3.0 Å distance cut off and 135° angle cut off.

| $X_{Aniline}$ | Distance (O..N) Å | Angle (∠O..H-N)° | % Occupancy | no of AN-AN H-bond |
|---|---|---|---|---|
| 0.05 | 2.886 | 157.5 | 21.5 | 0.22 |
| 0.13 | 2.886 | 158.5 | 39.6 | 1.53 |
| 0.74 | 2.886 | 158.5 | 47.1 | 17.7 |
| 1.0 | 2.882 | 158.8 | 44.5 | 26.9 |

Although, we have speculated that D-A H-bonding becomes favourable at some intermediate mole fractions in the presence of a non-interacting co-solvent in our previous works[5, 18] but it is for the first time, we explicitly show this here by MD simulation. The simulation indicates that cylohexane reduces D-D H-bonding and enhances D-A H-bonding at the intermediate mole fraction compared to neat aniline. Thus if PET is assisted by H-bonding the excess H-bonded D-A pairs may accelerate the net PET process and thus, surpasses the rate observed at neat condition. In fact a simulation with excited-state charge densities on C153 may give a better insight. However, if we take the view of Zhao and Han[9] that H-bonding becomes stronger in the excited state, we could expect an even more preferable distribution of the H-bonded species in the mixture compared to neat aniline.

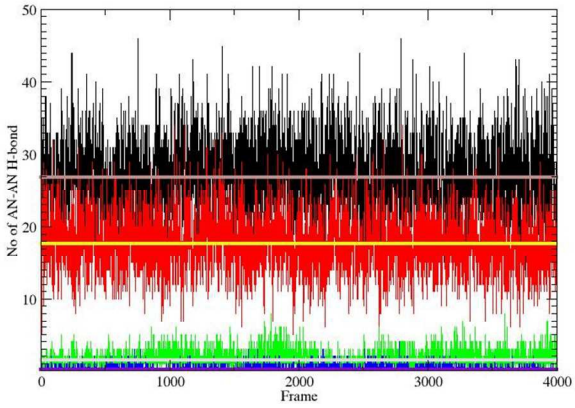


**Fig. 6** The variation of number of AN-AN H-bonding at different mole fractions of the mixture. The number of AN-AN bonding diminishes with decrease of the AN mole fraction. The average number of H-bonding is indicated by the solid lines.

## 4 Summary and Conclusions

In summary, using steady-state and ultrafast fluorescence measurements, we demonstrated that the PET behavior of an acceptor (C153) dissolved in mixture of an electron donor and a non-interacting solvent may be drastically different in nature depending on the possibility of H-bond formation with the acceptor. In the case of DMA, the co-solvent retards PET while the same co-solvent assists PET from aniline to C153 at some

particular composition of the mixture. FTIR measurements give the evidence of H-bond formation between C153 and aniline in the cyclohexane-aniline mixtures at all mole fractions. The speculation that H-bonding indeed assists the PET in aniline containing mixtures, is further rationalized from MD simulations. MD simulation revealed the presence of highest probability of C153-AN H-bonding at the same mole fraction where PET rate was found to be the fastest. This remarkable agreement between the experiments and theory confirms the theoretical predication that H-bonding should favor PET within the coumarin-aniline complex. Here, for the first time, we provide microscopic view that a passive solvent favors D-A H-bonding in a mixture at some definite mole fraction in comparison to neat aniline.

## Acknowledgements

This work is supported by Indian Institute of Technology Guwhati; the Council of Scientific and Industrial Research (CSIR), India (No 01/(2828)/15/EMR-II) and Department of Science and Technology, India (EMR/2014/00011). We thank Prof. Kankan Bhattachayya and his students (Rajdeep Chowdhury and Shyamtanu Chattoraj) for generous help in the fluorescence upconversion measurements.

## Notes and references

*Department of Chemistry, Indian Institute of Technology Guwahati, Guwahati 781039, Assam, India, Email: ksahu@iitg.ernet.in*

*†Electronic Supplementary Information (ESI) available: Composition of simulation mixtures; variation of density during simulation; Absorption spectra in cyclohexane-DMA mixture; FTIR spectra, Optimized structures of the H-bonded complex; Molecular orbital pictures, Chemical structures of C153, aniline and cyclohexane with atom label; rdf representing distribution of aniline around differnt H-bond accepting sites of C153; radial distribution function between C=O group of C153 and H atom of cyclohexane. See DOI: 10.1039/b000000x/*

## References

1. A. Shah, B. Adhikari, S. Martic, A. Munir, S. Shahzad, K. Ahmad and H.-B. Kraatz, *Chem. Soc. Rev.*, 2015, **44,** 1015-1027.

2. Y.-T. Long, E. Abu-Irhayem and H.-B. Kraatz, *Chem. Eur. J.*, 2005, **11,** 5186-5194.

3. E. Gatto, A. Quatela, M. Caruso, R. Tagliaferro, M. De Zotti, F. Formaggio, C. Toniolo, A. Di Carlo and M. Venanzi, *ChemPhysChem*, 2014, **15,** 64-68.

4. D. B. Bucher, A. Schlueter, T. Carell and W. Zinth, *Angew. Chem. Int. Ed.*, 2014, **53,** 11366-11369.

5. N. Barman and K. Sahu, *RSC Adv.*, 2014, **4,** 58299-58306.

6. N. Barman, D. Singha and K. Sahu, *J. Phys. Chem. A*, 2013, **117,** 3945-3953.

7. H. Shirota, H. Pal, K. Tominaga and K. Yoshihara, *J. Phys. Chem. A*, 1998, **102,** 3089-3102.

8. H. N. Ghosh, S. Verma and E. T. J. Nibbering, *J. Phys. Chem. A*, 2010, **115,** 664-670.

9. G.-J. Zhao and K.-L. Han, *J. Phys. Chem. A*, 2007, **111,** 2469-2474.

10. G.-J. Zhao, J.-Y. Liu, L.-C. Zhou and K.-L. Han, *J. Phys. Chem. B*, 2007, **111,** 8940-8945.

11. G.-J. Zhao and K.-L. Han, *Acc. Chem. Res.*, 2012, **45,** 404-413.

12. Y. Liu, J. Ding, D. Shi and J. Sun, *J. Phys. Chem. A*, 2008, **112,** 6244-6248.

13. Y.-H. Liu and P. Li, *J. Lumin.*, 2011, **131,** 2116-2120.

14. D. Yang, Y. Liu, D. Shi and J. Sun, *Comp. Theor. Chem.*, 2012, **984,** 76-84.

15. G.-J. Zhao and K.-L. Han, *J. Phys. Chem. A*, 2007, **111,** 9218-9223.

16. G.-J. Zhao and K.-L. Han, *Biophys. J.*, 2008, **94,** 38-46.

17. N. Barman, D. Singha and K. Sahu, *Phys. Chem. Chem. Phys.*, 2014, **16,** 6159-6166.

18. N. Barman and K. Sahu, *Phys. Chem. Chem. Phys.*, 2014, **16,** 27096-27103.

19. B. D. N. Rao, P. Venkateswarlu, A. S. N. Murthy and C. N. R. Rao, *Can. J. Chem.*, 1962, **40,** 963-965.

20. D. Schemmel and M. Schütz, *J. Chem. Phys.*, 2010, **132,** 174303.

21. E. W. Castner, D. Kennedy and R. J. Cave, *J. Phys. Chem. A*, 2000, **104,** 2869-2885.

22. R. Letrun and E. Vauthey, *J. Phys. Chem. Lett.*, 2014, **5,** 1685-1690.

23. D. K. Palit, T. Zhang, S. Kumazaki and K. Yoshihara, *J. Phys. Chem. A*, 2003, **107,** 10798-10804.

24. K. Yoshihara, K. Tominaga and Y. Nagasawa, *Bull. Chem. Soc. Jpn.*, 1995, **68,** 696-712.

25. H. Pal, Y. Nagasawa, K. Tominaga and K. Yoshihara, *J. Phys. Chem.*, 1996, **100,** 11964-11974.

26. K. Dobek, J. Karolczak and J. Kubicki, *Dyes and Pigments*, 2014, **100,** 222-231.

27. K. Sahu, S. Ghosh, S. K. Mondal, B. C. Ghosh, P. Sen, D. Roy and K. Bhattacharyya, *J. Chem. Phys.*, 2006, **125,** 044714-044718.

28. K. Sahu, S. K. Mondal, S. Ghosh, D. Roy, P. Sen and K. Bhattacharyya, *J. Phys. Chem. B*, 2005, **110,** 1056-1062.

29. M. J. T. Frisch, G. W.; Schlegel, H. B.; Scuseria, G. E.; Robb, M. A.; Cheeseman, J. R.; Montgomery, Jr., J. A.; Vreven, T.; Kudin, K. N.; Burant, J. C.; Millam, J. M.; Iyengar, S. S.; Tomasi, J.; Barone, V.; Mennucci, B.; Cossi, M.; Scalmani, G.; Rega, N.; Petersson, G. A.; Nakatsuji, H.; Hada, M.; Ehara, M.; Toyota, K.; Fukuda, R.; Hasegawa, J.; Ishida, M.; Nakajima, T.; Honda, Y.; Kitao, O.; Nakai, H.; Klene, M.; Li, X.; Knox, J. E.; Hratchian, H. P.; Cross, J. B.; Bakken, V.; Adamo, C.; Jaramillo, J.; Gomperts, R.; Stratmann, R. E.; Yazyev, O.; Austin, A. J.; Cammi, R.; Pomelli, C.; Ochterski, J. W.; Ayala, P. Y.; Morokuma, K.; Voth, G. A.; Salvador, P.; Dannenberg, J. J.; Zakrzewski, V. G.; Dapprich, S.; Daniels, A. D.; Strain, M. C.; Farkas, O.; Malick, D. K.; Rabuck, A. D.; Raghavachari, K.; Foresman, J. B.; Ortiz, J. V.; Cui, Q.; Baboul, A. G.; Clifford, S.; Cioslowski, J.; Stefanov, B. B.; Liu, G.; Liashenko, A.; Piskorz, P.; Komaromi, I.; Martin, R. L.; Fox, D. J.; Keith, T.; Al-Laham, M. A.; Peng, C. Y.; Nanayakkara, A.; Challacombe, M.; Gill, P. M. W.; Johnson, B.; Chen, W.; Wong, M. W.; Gonzalez, C.; and Pople, J. A., *Gaussian, Inc., Wallingford CT.*, 2004

30. U. C. Singh and P. A. Kollman, *J. Comput. Chem.*, 1984, **5,** 129-145.

31. L. Martínez, R. Andrade, E. G. Birgin and J. M. Martínez, *J. Comput. Chem.*, 2009, **30,** 2157-2164.

32. T. A. D. D.A. Case, T.E. Cheatham, III, C.L. Simmerling, J. Wang, R.E. Duke, R., R. C. W. Luo, W. Zhang, K.M. Merz, B. Roberts, S. Hayik, A. Roitberg, G. Seabra,, A. W. G. J. Swails, I. Kolossváry, K.F.Wong, F. Paesani, J. Vanicek, R.M.Wolf, J. Liu,, S. R. B. X. Wu, T. Steinbrecher, H. Gohlke, Q. Cai, X. Ye, J. Wang, M.-J. Hsieh, G., D. R. R. Cui, D.H. Mathews, M.G. Seetin, R. Salomon-Ferrer, C. Sagui, V. Babin, T. and S. G. Luchko, A. Kovalenko, and P.A. Kollman, 2012

33. J. Wang, R. M. Wolf, J. W. Caldwell, P. A. Kollman and D. A. Case, *J. Comput. Chem.*, 2004, **25,** 1157-1174.
34. J. Wang and T. Hou, *J. Chem. Theory Comput.*, 2011, **7,** 2151-2165.
35. J.-P. Ryckaert, G. Ciccotti and H. J. C. Berendsen, *J. Comput. Phys.*, 1977, **23,** 327-341.
36. W. Humphrey, A. Dalke and K. Schulten, *J. Mol. Graphics*, 1996, **14,** 33-38.
37. G. Jones, W. R. Jackson, C. Y. Choi and W. R. Bergmark, *J. Phys. Chem.*, 1985, **89,** 294-300.